

SHORT– AND MEDIUM–RANGE ORDER IN BISMUTH–SILICATE GLASSES: A MOLECULAR DYNAMICS STUDY

AGNIESZKA WITKOWSKA¹, JAROSŁAW RYBICKI¹,
ROBERT LASKOWSKI¹, GIORGIO MANCINI²,
SANDRO FELIZIANI², WITOLD ALDA³

¹*Department of Solid State Physics,
Faculty of Technical Physics and Applied Mathematics,
Technical University of Gdansk, Narutowicza 11/12, 80–952 Gdansk, Poland*

²*INFN UdR Camerino, Istituto di Matematica e Fisica,
Universita' di Camerino, via Madonna delle Carceri, Camerino (MC), Italy*

³*Institute of Computer Science, University of Mining and Metallurgy,
Mickiewicza 30, 30–059 Cracow, Poland*

Abstract: We report on the results of classical molecular dynamics (MD) simulations of structure of amorphous 15 Bi₂O₃ 85 SiO₂ [% mol] and 40 Bi₂O₃ 60 SiO₂ [% mol], and their totally reduced forms, 15 Bi₂ 85 SiO₂ [% mol], and 40 Bi₂ 60 SiO₂ [% mol], respectively. The simulations have been performed in the isobaric–isothermal ensemble, using a two–body interaction potential. The set of the potential parameters was constructed as a suitable combination of the parameters which were previously proposed for pure Bi₂O₃, and SiO₂. Both unreduced, and reduced systems were initially prepared as well equilibrated hot melts, and then slowly cooled down to 300K. The structural information from the MD simulations was obtained from radial and angular distribution functions, static structural factors, Voronoi polyhedra statistics, and ring analysis.

The simulation results can be summarised as follows. In unreduced glass with 15 Bi₂O₃ [%mol] contents, the silicon structural units (mainly regular tetrahedra) form continuous network, whereas in 40 Bi₂O₃ [%mol] glass these units are disconnected. In both unreduced systems Bi ions have mainly six–fold oxygen co–ordination, and no dominating structural unit can be individuated. However, the distorted bismuth units form a continuous network. In both totally reduced glasses (15 Bi₂ 85 SiO₂, and 40 Bi₂ 60 SiO₂ [% mol]), the silica network is built entirely from corner sharing SiO₄ tetrahedra. The structure of the silica subsystem is similar to that of pure α -SiO₂. After the reduction, the Bi–Bi co–ordination significantly increases, whereas the first neighbour distance decreases. Moreover, partial static structural factors for Bi–Bi pairs indicate that the medium–range order in reduced glasses exhibits greater periodicity than in unreduced glasses. Neutral Bi atoms form small clusters within the silica matrix.

Keywords: structure of matter, oxide glasses, MD simulation

1. Introduction

Bismuth glasses have been extensively investigated following the pioneering papers by Dumbaugh [1, 2]. Recently, interest in bismuth glasses has increased because of their high non-linear optical susceptibility [3], and their ability to synthesise high temperature ceramic superconductors [4, 5]. For example, bismuth-silicate glasses of composition $x\text{Bi}_2\text{O}_3$ (100- x) SiO_2 ($x \geq 40$ [% mol]) are of particular interest because of their applicability in production of low-loss fibre optic materials in the infrared region [6], and also as the active medium of Raman-active fibre optical amplifiers [7]. However, the structural role played by Bi_2O_3 in such non-conventional glasses is complicated and poorly understood. The problem is so complex because crystalline Bi_2O_3 can form several polymorphs with highly distorted corner-, and edge-sharing polyhedra [8, 9].

The present contribution is dedicated to a molecular dynamics study of the structure of bismuth-silicate glasses of compositions 15 Bi_2O_3 85 SiO_2 [% mol] and 40 Bi_2O_3 60 SiO_2 [% mol]. The value of $x = 40$ is the lower bound on the appearance of continuous bismuth oxide network [12]. Moreover, the bismuth-silicate glasses are known to undergo dramatic changes of optical properties [10] and electrical surface conductivity [11], when submitted to the hydrogen reduction process. Since these changes must be related to the structural reconstruction of the material, we have also performed the simulations of totally reduced 15 Bi_2 85 SiO_2 [% mol] and 40 Bi_2 60 SiO_2 [% mol] glasses. In Section 2 we describe in brief the applied simulation technique and the methods of structural analysis of the obtained atom configurations. The simulation results are described, discussed, and compared to the available experimental data in Section 3. Section 4 contains concluding remarks.

2. Simulation technique

The molecular dynamics (MD) method is at present widely used for structural modelling. It consists in numerical solution of the classical many-body problem of interacting particles, so that the trajectories of all particles within a simulation box are found. At this point the laws of statistical physics are operative, that is, suitable averaging procedures over the atom trajectories yield the structural and thermodynamical information on the system (*e.g.* [13]).

The simulations have been performed in the isobaric-isothermal (NpT) ensemble according to the Andersen algorithm [14]. The atoms were assumed to interact by a two-body potential (Born-Mayer repulsive forces, and Coulomb forces due to full ionic charges, calculated with the aid of the standard Ewald technique), with Si-Si, Si-O, and O-O interactions parametrised by Soules [15]. The Bi-Bi interaction parameters have been taken from [16], and Bi-O, and Bi-Si interaction parameters have been calculated as suitable averaging of Bi-Bi and O-O, and Bi-Bi, and Si-Si interactions. Our potential parametrisation was tested in the range of the glass compositions $x = 15 \div 60$. It allows to perform successfully the MD simulations at zero external pressure in the considered range of stoichiometries, both

of unreduced, and totally reduced (for $x \leq 50$) glasses. All the systems discussed in the present work were initially prepared in a well equilibrated molten state at 6000K, and then slowly cooled down to 300K, passing equilibrium states at 5000K, 4000K, 3000K, 2500K, 2000K, 1500K, 1000K, 600K. At each temperature the system was being equilibrated during 30000 fs time steps, and sampled during other 10000 time steps. The numbers of atoms within the simulation box are summarised in Table I.

The structural information from the MD-simulated equilibrium final

Table I. Numbers of atoms within the simulation box.

	$x = 15,$ <i>unreduced</i>	$x = 15,$ <i>reduced</i>	$x = 40,$ <i>unreduced</i>	$x = 40,$ <i>reduced</i>
Bi	300	300/3000	400	400/6000
Si	850	850/8500	300	300/4500
O	2150	1700/17000	1200	600/9000

configuration of N atoms was obtained from radial ($g_{\alpha\beta}(r)$) and angular distribution functions, and static structural factors, calculated from the radial distribution function as:

$$S_{\alpha\beta}(k) = \delta_{\alpha\beta} + 4\pi(c_{\alpha}c_{\beta})^{1/2} \int_0^{\infty} [g_{\alpha\beta}(r) - 1] \frac{\sin(kr)}{kr} r^2 dr ,$$

where α and β label the atom types, $\delta_{\alpha\beta}$ is the Kronecker symbol, and c_{α} , c_{β} are the relative concentrations of α , and β atoms, respectively. Also other, more advanced structure analysis methods based on new algorithms were applied. In particular we have performed the stochastic geometry analysis (Voronoi polyhedra) [17–18], and the cation–anion ring analysis [19–23].

The Voronoi polyhedron (VP) is defined as the minimal polyhedron whose planar faces bisect at right angles to the lines joining an atom to its neighbours. The VP network (a set of VP constructed for all atoms in the sample) splits in a unique manner the total sample volume into the zones owned by each atom. VP network contains the whole information about the structure of the sample. The shape of a VP reflects the arrangement of all the neighbours of a given atom. In the amorphous structures VPs are rather complex polyhedrons. Our Voronoi analysis was performed using the recent developments of the method [17, 18].

An X–O–X–O... ring with N X cations is called N -member ring. In our cation–anion ring analysis the ring detection was performed using a new highly efficient redundance aware algorithm. It follows the general guidelines of Balducci and Pearlman [21] message passing method, but a new approach based on a pre-filtering technique is introduced to perceive rings in structures represented by 2-connected graphs [23].

3. Simulation results and discussion

Table II summarises the obtained average nearest neighbour distances and co-ordination numbers. Figures 1–4 show radial, and several angular distribution functions, respectively. The figures refer to the equilibrium structure of samples cooled slowly down to 300K. Curves (a) correspond to unreduced systems, whereas curves (b) refer to the totally hydrogen reduced systems. We shall now discuss in turn the structure of the silicate subsystem (Section 3.1), and the bismuth subsystem (Section 3.2).

Table II. The first neighbour distances, and the first co-ordination numbers (in brackets) for unreduced and totally reduced glasses.

	15%, unreduced	15%, reduced	40%, unreduced	40%, reduced
Bi – Bi [A]	4.12 [2.6]	3.96 [4.0]	4.22 [4.1]	3.78 [8.2]
Bi – Si [A]	3.96 [6.4]	4.18 [9.2]	3.78 [5.2]	3.92 [2.6]
Si – Bi [A]	3.96 [2.3]	4.18 [3.3]	3.78 [6.9]	3.92 [3.4]
Bi – O [A]	2.62 [5.7]	3.70 [11.1]	2.64 [6.2]	3.40 [1.95]
O – Bi [A]	2.62 [0.9]	3.70 [1.2]	2.64 [2.1]	3.40 [1.3]
Si – Si [A]	3.26 [3.2]	3.26 [4.01]	3.30 [1.4]	3.20 [4.0]
Si – O [A]	1.64 [4.1]	1.66 [4.0]	1.62 [4.4]	1.62 [4.0]
O – Si [A]	1.64 [1.6]	1.66 [2.0]	1.62 [1.1]	1.62 [2.0]
O – O [A]	2.62 [4.9]	2.62 [6.2]	2.60 [3.5]	2.60 [6.3]

3.1. Silica subsystem

The inspection of radial Si–O and O–O distribution functions (Figure 1 and 3), and of angular O–Si–O and O–O–O distribution functions (Figure 2 and 4) indicates that the first co-ordination shell of silicon ion in unreduced glasses consists mainly of four oxygen ions. Detailed counting of neighbouring oxygen atoms around Si atoms confirms the latter fact (Table III). Four-fold co-ordinated Si remains in the centre of a regular tetrahedron, whereas five-fold co-ordinated Si remains approximately in the centre of the basis of a regular square pyramid. The SiO₄ tetrahedra are somewhat more distorted for $x = 40$ glass. Significant difference in the structure of the silica subsystem between the two compositions is seen in the network continuity. For $x = 15$ we observe continuous network, containing a significant fraction of long rings (up to 16-member rings, Figure 5A). Thus, the structure is rather an open one. In the case of $x = 40$ the silicon structural units do not form any continuous network. We have constructed an adjacency graph for this composition, setting on a Si–O bond if the distance between silicon and oxygen atoms was shorter than 0.2 nm (using periodic boundary conditions). The obtained graph was highly disconnected, composed of over one hundred small connected subgraphs, mainly stars, and bi-stars.

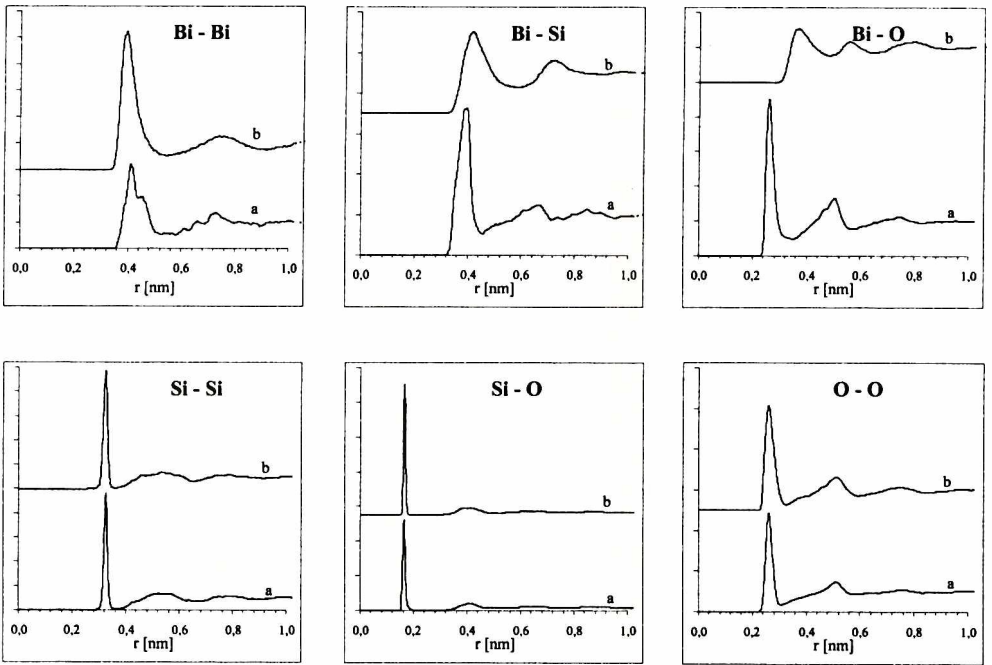


Figure 1. Radial distribution functions in unreduced $15 \text{ Bi}_2\text{O}_3, 85 \text{ SiO}_2$ [% mol] glass (curves a), and totally reduced $15 \text{ Bi}_2, 85 \text{ SiO}_2$ [% mol] glass (curves b)

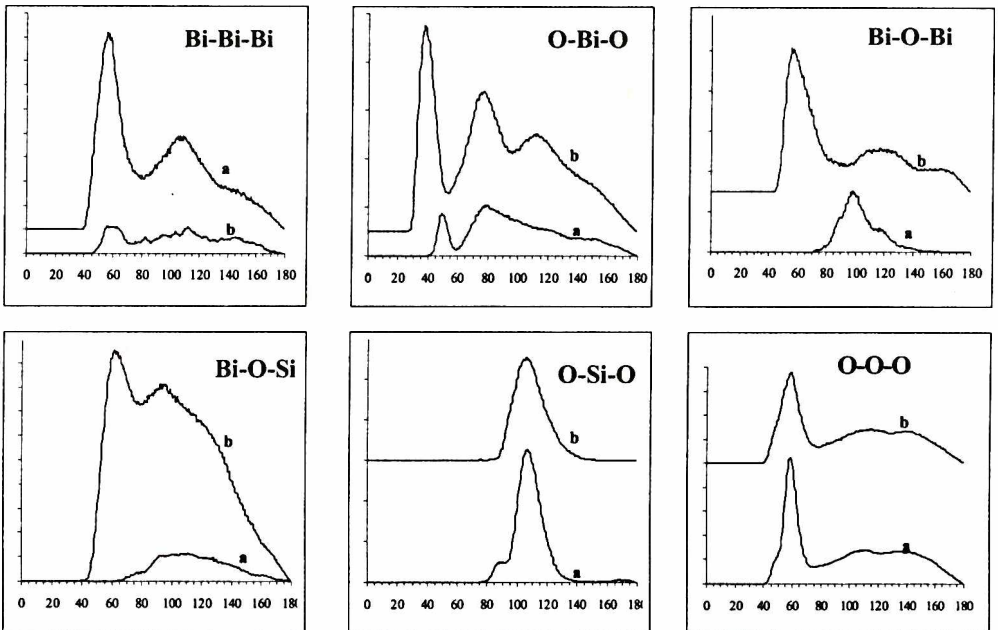


Figure 2. Angular distribution functions in unreduced $15 \text{ Bi}_2\text{O}_3, 85 \text{ SiO}_2$ [% mol] glass (curves a), and totally reduced $15 \text{ Bi}_2, 85 \text{ SiO}_2$ [% mol] glass (curves b)

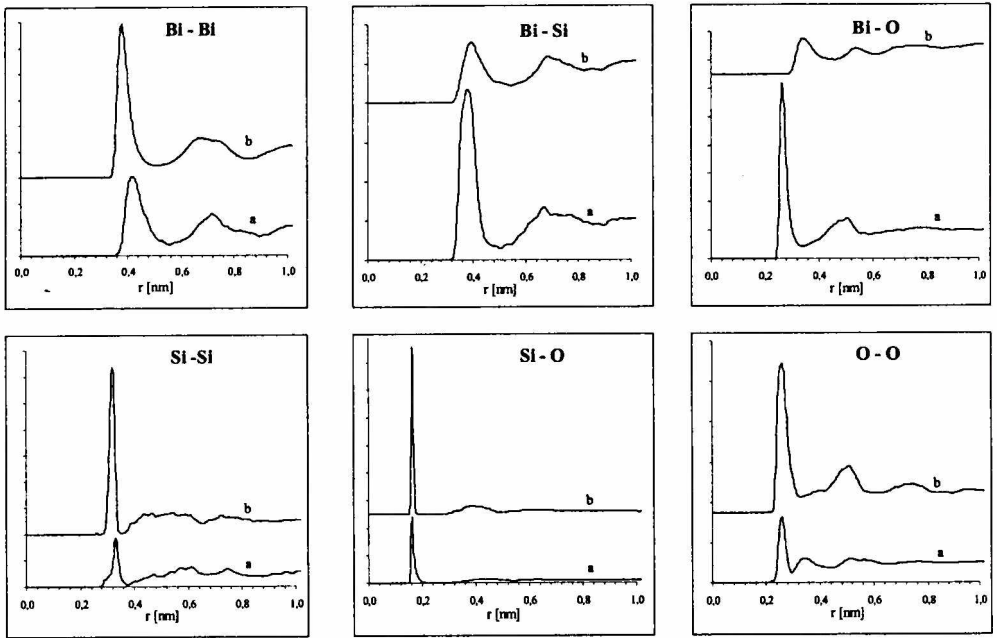


Figure 3. Radial distribution functions in un-reduced 40 Bi_2O_3 , 60 SiO_2 [% mol] glass (curves a), and totally reduced 40 Bi_2 , 60 SiO_2 [% mol] glass (curves b)

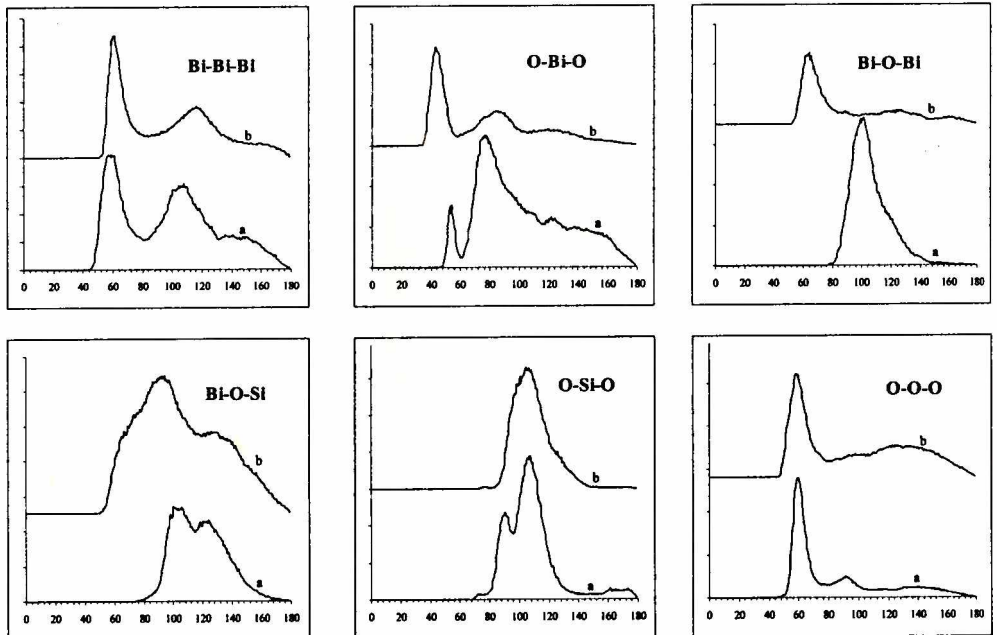


Figure 4. Angular distribution functions in un-reduced 40 Bi_2O_3 , 60 SiO_2 [% mol] glass (curves a) and totally reduced 40 Bi_2 , 60 SiO_2 [% mol] glass (curves b)

Table III. The statistics of the first co-ordination shell of silicon atoms in unreduced glasses.

Oxygen co-ordination of Si atoms	15 Bi ₂ O ₃ [% mol]	40 Bi ₂ O ₃ [% mol]
4-fold	91%	70%
5-fold	9%	28.5%
6-fold	—	1.5%

In the reduced systems, $x\text{Bi}_2(100-x)\text{SiO}_2$ ($x = 15, 40$ [% mol]), the structure of the silica subsystem is quite different. All the silicon ions are co-ordinated with four oxygen atoms, and the only silica structural unit is a regular tetrahedron. In contradistinction to the case of unreduced system, here we have obtained for both glass compositions a silica network formed entirely from corner-sharing SiO_4 tetrahedra. Thus, the structure of the silica subsystems is similar to that of pure vitreous SiO_2 , which also consists of random network of corner-sharing tetrahedra. The difference between the silica network in pure $\alpha\text{-SiO}_2$ and in the Bi doped the SiO_2 networks can be seen in the ring statistics. Various models of well-relaxed pure vitreous SiO_2 contain predominantly five-, six-, and seven-member rings [24, 25]. The occurrence of smaller rings geometrically constrains the relaxation of the network. The extreme is a two-member ring, in silica corresponding to edge sharing tetrahedra. Three-member rings do not occur in any pure SiO_2 polymorph, but they do exist in some silicate minerals, where the Si-O-Si-O-Si-O rings form anionic cages for various cations. In bulk vitreous SiO_2 two- and three-member rings are considered as defects. The distribution of silicon-oxygen ring lengths in our

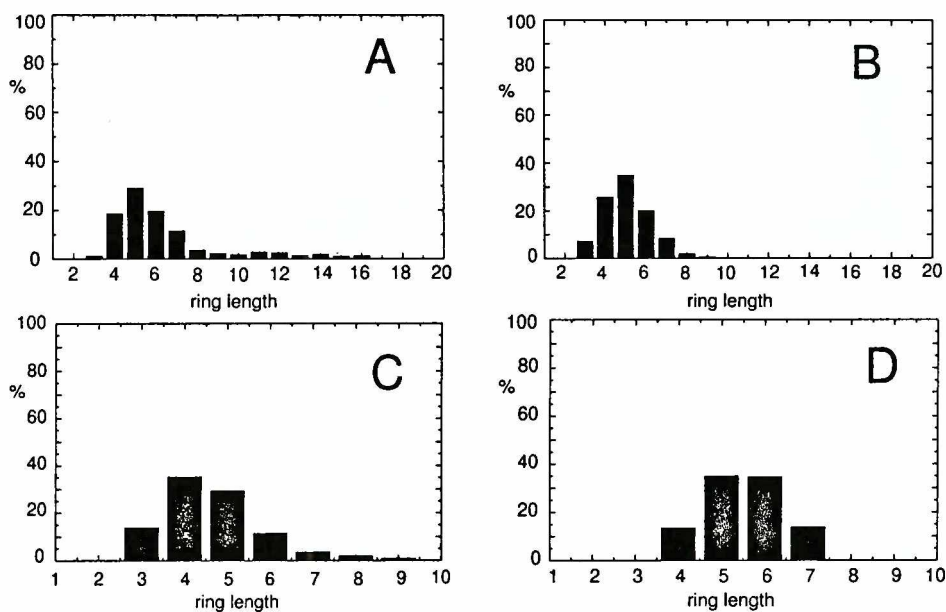


Figure 5. Si-O-Si-O... ring length distribution in unreduced 15 Bi₂O₃ 85 SiO₂ [% mol] (A), totally reduced 15 Bi₂ 85 SiO₂ [% mol] (B), totally reduced 40 Bi₂ 60 SiO₂ [% mol] (C), and in pure silica (D)

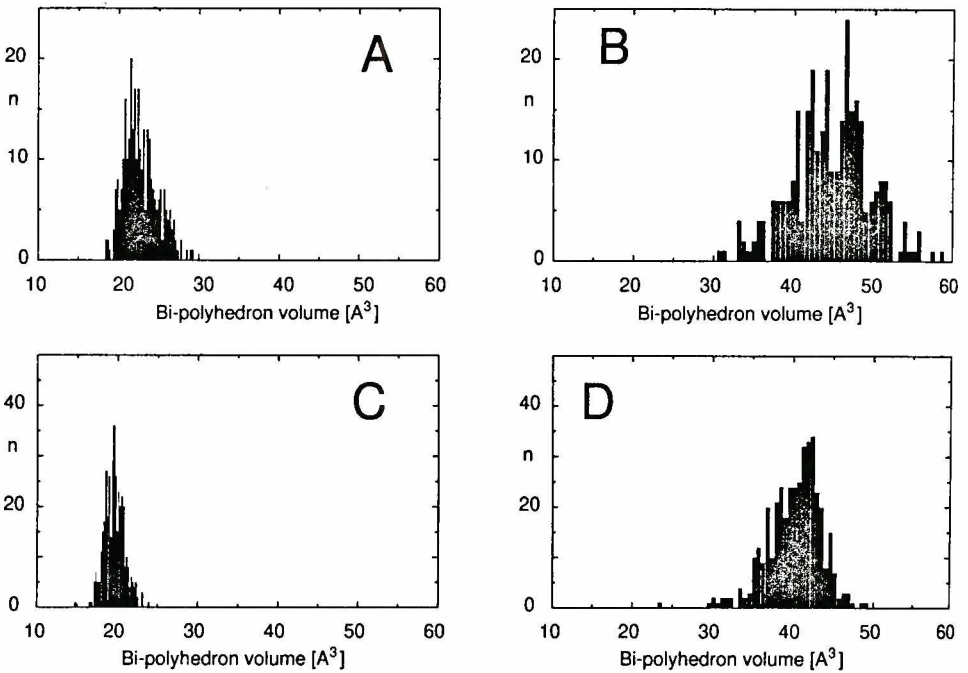


Figure 6. Distribution of the volumes [\AA^3] of the Voronoi polyhedra centred on Bi atoms. (A) – 15 Bi_2O_3 , 85 SiO_2 [% mol]; (B) – 15 Bi, 85 SiO_2 [% mol]; (C) – 40 Bi_2O_3 , 60 SiO_2 [% mol]; (D) – 40 Bi_2 , 60 SiO_2 [% mol]

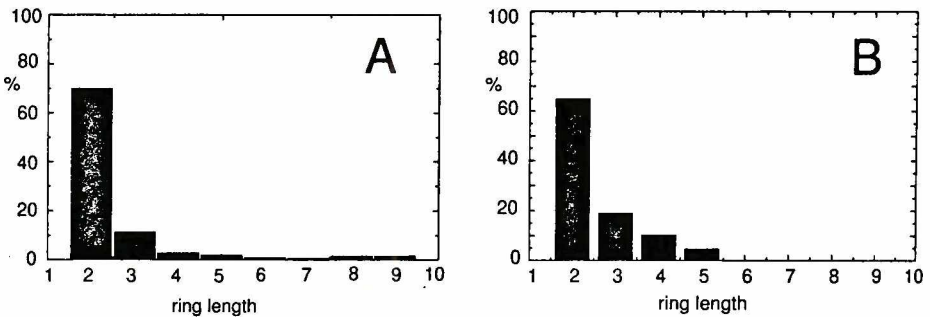


Figure 7. Bi-O-Bi-O... ring length distribution in unreduced glasses for $x = 15$ (A), and $x = 40$ (B)

neutral-bismuth containing glasses is shown in Figure 5B and Figure 5C. For comparison, in Figure 5D we show the distribution of silicon–oxygen ring lengths in pure SiO_2 glass simulated with the same potential. As it is seen, the silica networks of our reduced bismuth glasses contain more defects than pure silica (3-fold rings), the contribution of well relaxed rings (6-, and 7-fold) is significantly lower, and the percentage of strained 4-fold rings is higher. As expected, the silica network in the reduced $x = 15$ glass is more similar to the pure α - SiO_2 network, than that of the $x = 40$ glass (about 62%, and 41% of 5-, 6-, and 7-member rings, for $x = 15$, and $x = 40$, respectively).

3.2. Bismuth subsystem

Some experimental structural data are available for α -phase of crystalline Bi_2O_3 [26] and crystalline $\text{Bi}_4\text{Si}_3\text{O}_{12}$ [27]. These data are to be compared with our simulation results for the unreduced glass. As far as the authors know, no experimental data on atomic level have been published for reduced bismuth-silicate glasses, and thus in this case only simulation results will be presented.

According to [26] the total co-ordination number of Bi^{3+} ions in the radial range $0.21 \div 0.27$ nm in the α -phase of crystalline Bi_2O_3 is close to five. One of the Bi–O bonds (the shortest one) is $0.206 \div 0.21$ nm long. The remaining four Bi–O bonds are approximately classified into two shorter distances ($0.22 \div 0.23$ nm) and two longer distances ($0.24 \div 0.27$ nm). In addition, there is another Bi–O distance about 0.28 nm long, which increases the co-ordination number to six. In the crystalline $\text{Bi}_4\text{Si}_3\text{O}_{12}$ [27] three Bi–O bonds are about 0.215 nm long, and other three — about 0.262 nm. In our MD simulated glasses the average Bi–O co-ordination number equals 5.7 and 6.2 for $x = 15$, and $x = 40$, respectively (Table IV). The Bi–O distance, as results from the width of the first RDF peak, ranges from 0.24 nm to 0.28 nm for both systems. The first Bi–O peaks have their maximum at 0.262 nm and at 0.264 nm, respectively (Table I). The nearest O–O distances range from 0.27 nm to 0.3 nm in $-\text{Bi}_2\text{O}_3$ [26], and from 0.262 nm to 0.315 nm in the crystalline form of $\text{Bi}_4\text{Si}_3\text{O}_{12}$ [27], which is also very similar to our result. For O–O bond length we obtained 0.262 nm for $x = 15$, whereas for $x = 40$, 0.26 nm and 0.34 nm. The oxygen neighbours of Bi ions determine a variety of distorted polyhedra difficult to classify. The distributions of the Bi–polyhedra volumes in both unreduced glasses are shown in Figures 6A, and 6C. As it is seen, the dispersion of the volumes owned by Bi ions is significantly lower in the 40 Bi_2O_3 [% mol] glass. The bismuth structural units form a continuous edge sharing network. This results from the Voronoi analysis, and is also seen from the Bi–O–Bi–O... ring statistics: two-member rings are the most frequent ones (about 70% — Figure 7A and about 67% — Figure 7B). In the glass with lower Bi_2O_3 concentration ($x = 15$) several longer rings have been perceived (8-, and 9-member rings). The average Bi–Bi distance amounts to 0.38 nm in Bi_2O_3 [26], and to 0.3875 nm in $\text{Bi}_4\text{Si}_3\text{O}_{12}$ [28]. In our simulations we have obtained significantly higher Bi–Bi distance — 0.412 nm, with the co-ordination equal to 2.6 for 15 Bi_2O_3 85 SiO_2 glass and 0.422 nm, with the co-ordination equal to 4.1 for 40 Bi_2O_3 60 SiO_2 glass.

Table IV. The statistics of the first co-ordination shell of bismuth atoms in unreduced glasses

Oxygen co-ordination of Bi atoms	15 Bi_2O_3 [% mol]	40 Bi_2O_3 [% mol]
4-fold	6%	—
5-fold	39.5%	20%
6-fold	39%	50.5%
7-fold	14%	25.3%
8-fold	1.5%	4.2%

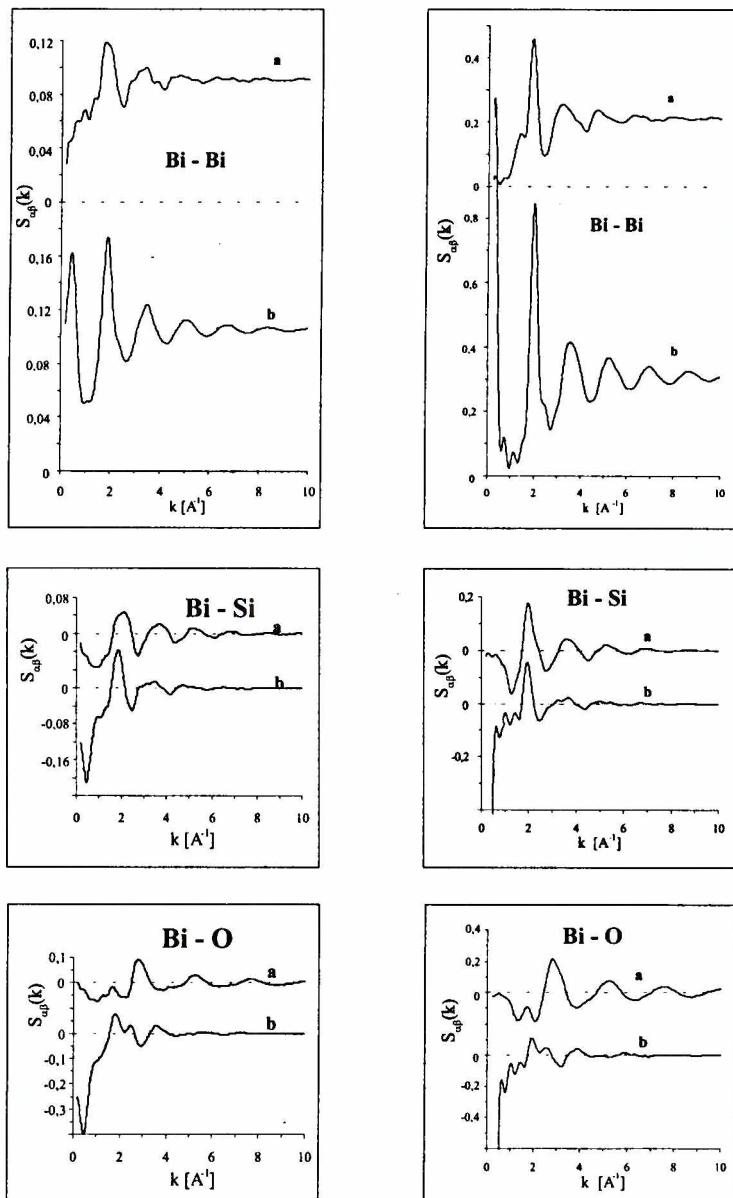


Figure 8. Partial static structural factors for Bi-Bi, Bi-Si, and Bi-O pairs for $x = 15$ (left figures), and $x = 40$ (right figures). Curves a: unreduced glasses, curves b: reduced glasses

On reduction, the structure of the bismuth subsystem undergoes remarkable changes. First of all, the first neighbour distances and the first co-ordination numbers both for the Bi-Bi pair, and for the Bi-O pair, change significantly. In comparison with the results for unreduced sample, the Bi-Bi distance decreases (by about 0.016 nm, and 0.044 nm for $x = 15$, and $x = 40$, respectively). At the same

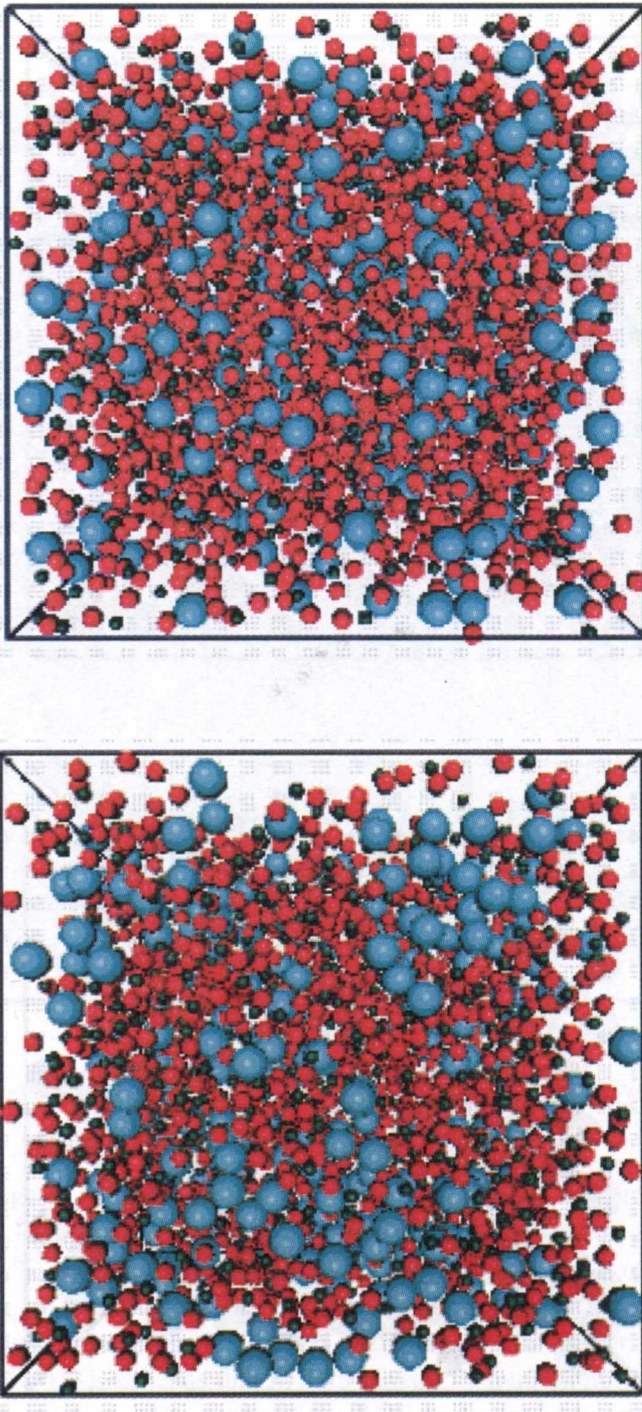


Figure 9. Distribution of atoms within the simulation box at the last simulation time-step in unreduced (left) and in reduced (right) glass (blue-bismuth, green-silicon, red-oxygen). The simulation boxes contain 3300, and 2850 atoms, respectively; $x = 15$

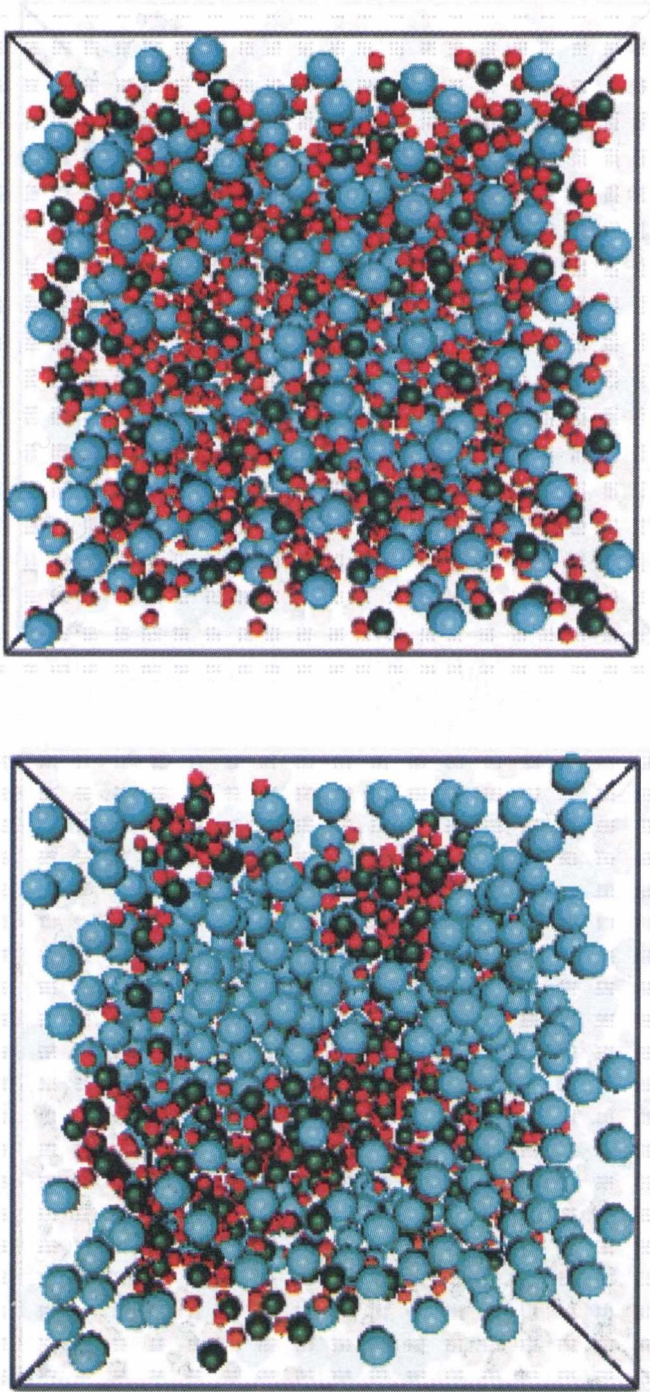


Figure 10. Distribution of atoms within the simulation box at the last simulation time-step in unreduced (left) and in reduced (right) glass (blue-bismuth, green-silicon, red-oxygen). The simulation boxes contain 1900, and 1300 atoms, respectively; $x = 40$

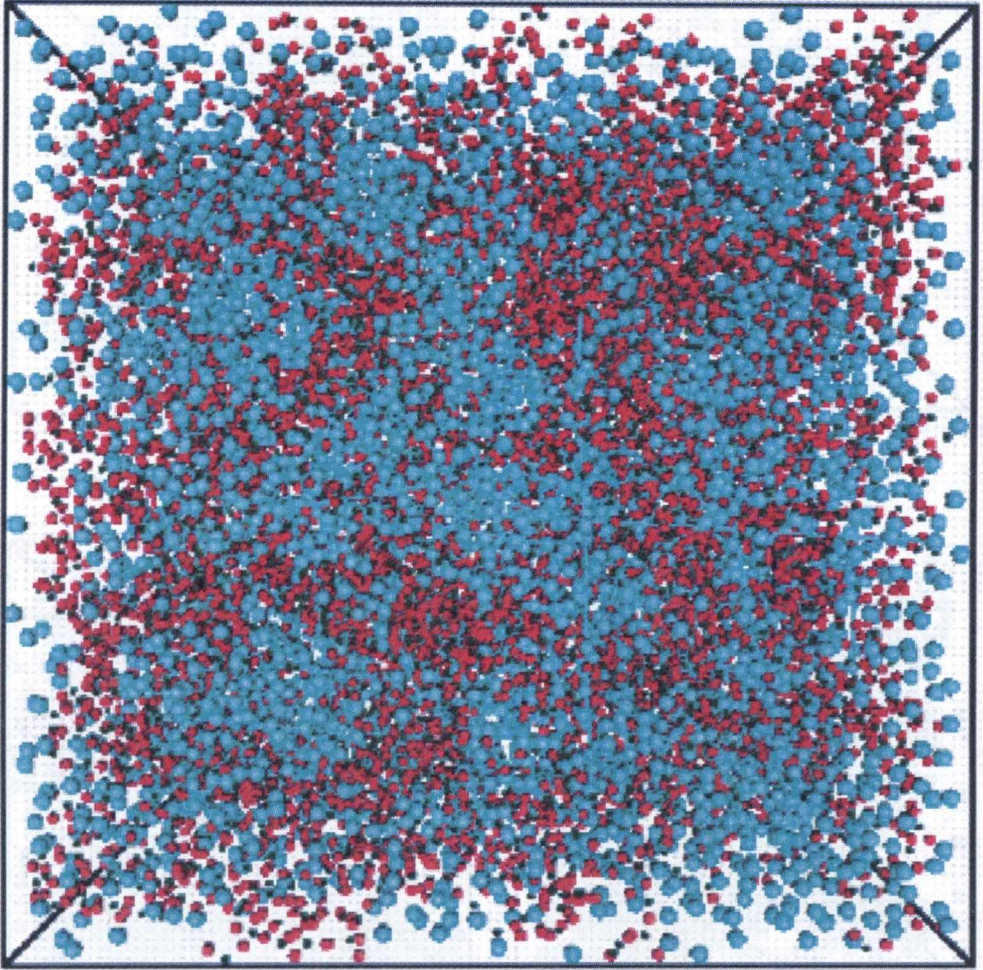
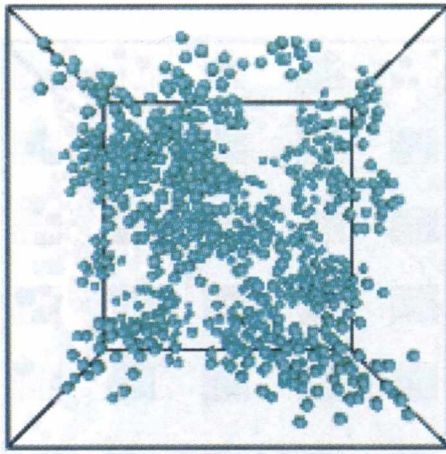


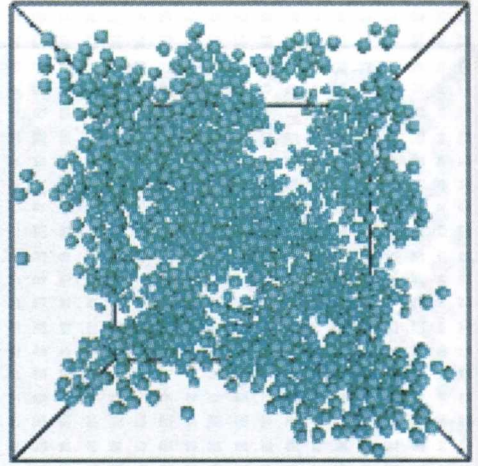
Figure 11. Distribution of atoms within the simulation box at the last simulation time-step in reduced glass (blue-bismuth, green-silicon, red-oxygen), $x = 40$. The simulation box contains 19500 atoms

time the average Bi–Bi co-ordination increases in both systems almost by the factor of two (Table I). The average Bi–O distances behave quite inversely: they increase by about 41% and about 29% for $x = 15$, and $x = 40$, respectively. The corresponding co-ordination number significantly increases in the case of the lower Bi concentration (from 5.7 to 11.1), and decreases for the higher Bi concentration (from 6.2 to 1.95). This means that in both glasses bismuth atoms agglomerate, and form granular structures. The shape of the RDF peaks, and the structure of the $S(k)$ peaks (Figure 8) confirm this conclusion. The Bi atom distributions in the unreduced, and reduced glasses are visualised directly in Figures 9–11.

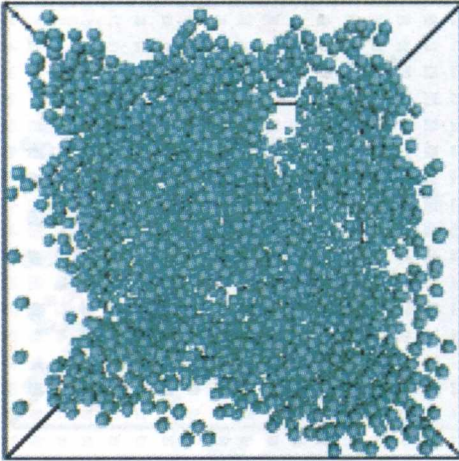
The bismuth granules seen in reduced samples (Figures 9–11) form a continuous network. In each case, the adjacency matrix for Bi subsystem represents a single



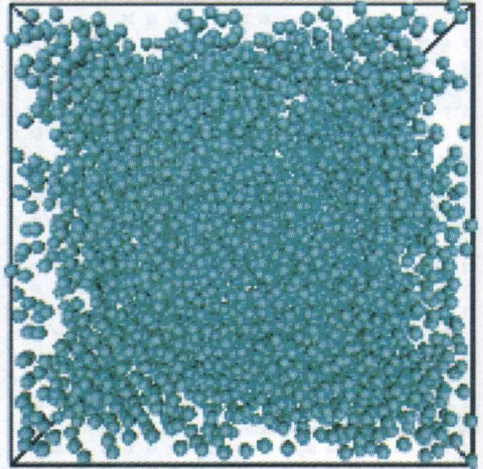
co-ordination ≥ 12



co-ordination ≥ 10



co-ordination ≥ 8



all atoms

Figure 12. Distributions of Bi atoms of given Bi-Bi co-ordination

cluster. Table V shows the distribution of Bi-Bi co-ordination numbers in our MD-simulated reduced glasses. Figure 12 shows spatial distributions of Bi atoms in the simulation box. The last panel presents all the Bi atoms, whereas three first panels present the Bi atoms with Bi-Bi co-ordination higher than or equal 12, 10, and 8, respectively. Thus, more and more low-co-ordinated atoms are eliminated. The last panel shows only the atoms fully surrounded by other Bi atoms. As it is seen, even such inner atoms of the granules have a rather continuous distribution, which means that the system of metal granules is highly connected.

Table V. Distribution of Bi-Bi co-ordination numbers in reduced glasses.

<i>Bi-Bi co-ordination</i>	<i>15% Bi₂ 85% SiO₂ 300 Bi atoms</i>	<i>40% Bi₂ 60% SiO₂ 400 Bi atoms</i>	<i>40% Bi₂ 60% SiO₂ 6000 Bi atoms</i>
1-fold	7%	0.25%	0.35%
2-fold	11%	0.5%	0.42%
3-fold	16.67%	0.75%	1.48%
4-fold	19.33%	2.75%	2.52%
5-fold	12.67%	5%	4.33%
6-fold	15.67%	7.75%	7.18%
7-fold	9.33%	7%	10.42%
8-fold	5%	9.5%	13.1%
9-fold	2.33%	13%	14.52%
10-fold	0.67%	15%	13.18%
11-fold	—	12%	13.17%
12-fold	0.33%	14.25%	11.35%
13-fold	—	9%	6.02%
14-fold	—	3.25%	1.63%
15-fold	—	—	0.27%
16-fold	—	—	0.07%

4. Conclusions

In the present work a parametrisation of a two body interaction potential for $x\text{Bi}_2\text{O}_3$ (1- x) SiO_2 [% mol] glasses has been proposed and tested in the range of the glass compositions $x = 15 \div 60$. Our potential allows to perform successfully the simulations at zero external pressure in the considered range of stoichiometries, both of unreduced, and totally reduced (for $x \leq 50$) glasses. The obtained interatomic distances, and co-ordination numbers agree well with the experimental data on unreduced glasses. As far as the authors know, there are no published experimental data on the atomic structure of totally reduced glasses, and so our simulations constitute the first study of the structure of reduced bismuth-silicate glasses. In accordance with the experiment, a strong tendency of neutral Bi atoms to form metal granules has been perceived, independently of the Bi_2O_3 contents. In contradistinction to the behaviour of the Pb atoms in reduced lead-silicate glasses, where great and separated metallic droplets appear [29], in our bismuth-silicate glasses strongly connected network of Bi clusters is formed within the silica matrix. In order to elucidate the kinetics of the metallic cluster formation much more extensive MD studies on $x\text{Bi}_2\text{O}_3$ (1- x) SiO_2 glasses and $x\text{Bi}_2\text{O}_3$ (1- x) GeO_2 glasses are in progress.

Acknowledgement

The opportunity to perform our simulations at the TASK Computer Centre in Gdansk (Poland), and at the Camerino University, Italy (grant 96.00844.ST76) is kindly acknowledged. The work has been partially supported by KBN, grant 2P03B 167 10.

References

- [1] Dumbaugh W., 1978, *Phys. Chem. Glasses*, **19** 121
- [2] Dumbaugh W., 1986, *Phys. Chem. Glasses*, **27** 119
- [3] Hall D., Newhouse N., Borrelli N., Dumbaugh W., Weidman D., 1989, *J. Appl. Phys. Lett.* **54** 1293
- [4] Komatsu T., Matusita K., 1991, *Thermochim. Acta*, **174** 131
- [5] Zheng H., Lin P., Xu R., Mackenzie J., 1990, *J. Appl. Phys.*, **68** 894
- [6] Nassau K., Chadwick D. L., Miller A. E., 1987, *J. Non-Cryst. Solids*, **93** 115
- [7] Lin C., 1983, *J. Opt. Commun.*, **4** 2
- [8] Dimitriev Y., Wright A. C., Mihailova V., Gattef E., Guy C. A., 1995, *J. Mat. Sci. Lett.*, **14** 347
- [9] Gattow G., Schroder H., 1962, *Z. Annorg. Allg. Chem.*, **318** 176
- [10] Heynes M. S. R., Rawson H., 1957, *J. Soc. Glass Technol.*, **41** 347
- [11] Pan Z., Henderson D. O., Morgan S. H., 1994, *J. Non-Cryst. Solids*, **171** 134
- [12] Trzebiatowski K., Murawski L., Kościelska B., Chybicki M., Gzowski O., Davoli I., 1997, *Proc. of the Conf. on Fundamental of Glass Science and Technology*, June 9–12, 1997, Vaxjo, Sweden
- [13] Rapaport D. C., 1995, *The Art of Molecular Dynamics Simulation*, Cambridge University Press
- [14] Andersen H. C., 1980, *J. Chem. Phys.*, **72** 2384
- [15] Soules T. F., 1982, *J. Non-Cryst. Solids*, **49** 29
- [16] Abrahamson A. A., 1969, *Phys. Rev.*, **178** 76
- [17] Laskowski R., Rybicki J., Chybicki M. 1997, *TASK Quart: Sci. Bull. Acad. Comp. Centre in Gdansk*, **1** 89
- [18] Brostow W., Laskowski R., Rybicki J., Chybicki M., 1998, *Phys. Rev.*, **B 57** 13448
- [19] Horton J. D., 1987, *SIAM J. Comp.*, **16** 358
- [20] Downs G. M., Gillet V. J., Holiday J. D., Lynch M. F., 1989, *J. Chem. Inf. Comput. Sci.*, **29** 172
- [21] Balducci R., Pearlman R. S., 1994, *J. Chem. Inf. Comput. Sci.*, **34** 822
- [22] Kaveh A., Roosta G. R., 1994, *Com. Num. Meth. Eng.*, **10** 525
- [23] Mancini G., 1997, *TASK Quart: Sci. Bull. Acad. Comp. Centre in Gdansk*, **1** 89
- [24] King S. V., 1967, *Nature*, **213** 1112
- [25] Hamann D. R., 1997, *Phys. Rev.*, **B 55** 14784
- [26] Malmros G., 1970, *Acta Chem. Scand.*, **24** 384
- [27] Segal D. J., Santoro R. P., Newnham R. E., 1966, *Z. Kristallogr.*, **123** 73
- [28] Harving H., 1978, *Z. Anorg. Allg. Chem.*, **444** 151
- [29] Rybicka A., Chybicki M., 1998, *Proc. of the Fourth Seminar on Porous Glasses Special Glasses*, October 2–5 1998, Szklarska Poręba, Ceramics **57** 135